ESC European Society of Cardiology

European Journal of Heart Failure (2026) **00**, 1–10
https://doi.org/10.1093/ejhf/xuag112

RESEARCH ARTICLE

Dyssynchronous heart failure: mitochondrial distribution and functions mirror regional workload and energy demand in a large-animal model of ventricular desynchronization

Alexander Dietl [1,*], Sabine Iberl[1], Lisa Marie Köhler[1], Katja Evert[2], Maria Heinrich[1], Esther Dreier[1], Jan Dudek [3], Christoph Magnes[4], Moritz Mayer[1], Michael Paulus [1], Christian Riehle[5], Stefan Wagner [1], Elmar Zügner[4], Lars S. Maier[1], Filip Rega[6,7], Christoph Maack [3,8], Alexander Nickel[3], Jens-Uwe Voigt[6,9,†], and Jürgen Duchenne[6,9,10,11,†]

[1]Department of Internal Medicine II, University Hospital Regensburg, Regensburg D-93042, Germany; [2]Institute of Pathology, University of Regensburg, Regensburg, Germany; [3]Department of Translational Research, Comprehensive Heart Failure Center (CHFC), University Hospital Wuerzburg, Wuerzburg, Germany; [4]Joanneum Research Health, Graz, Austria; [5]Department of Cardiology and Angiology, Hannover Medical School, Hannover, Germany; [6]Department of Cardiovascular Sciences, KU Leuven, Leuven, Belgium; [7]Department of Cardiothoracic Surgery, University Hospitals Leuven, Leuven, Belgium; [8]Medical Clinic and Polyclinic I, University Hospital Wuerzburg, Wuerzburg, Germany; [9]Department of Cardiovascular Diseases, University Hospitals Leuven, Leuven, Belgium; [10]Research Group Cardiology & Organ Systems, UHasselt, Diepenbeek, Belgium; and [11]Department of Cardiology, Heart Center Hasselt, Jessa Hospital, Hasselt, Belgium

Received 10 July 2025; revised 28 November 2025; accepted 2 March 2026; online publish-ahead-of-print 12 April 2026

Abstract

Aims

In dyssynchronous heart failure (DHF), left bundle branch block (LBBB) causes inhomogeneous left ventricular (LV) workload and systolic dysfunction. We aimed to investigate underlying metabolic remodelling in an ovine model.

Methods and results

Eleven sheep with dual-chamber-pacemakers for LBBB-like activation (DHF) were studied at baseline and after eight weeks. Six untreated sheep served as controls (CTRL). Regional workload was evaluated using invasive hemodynamics and echocardiography. 18F-fluorodeoxyglucose-tracer positron-emission-tomography/computed tomography visualized regional glucose-uptake. Magnetic resonance imaging assessed fibrosis (late gadolinium enhancement, LGE). Septal and lateral wall tissue was analysed with histology, confocal microscopy, ultra-high-performance liquid chromatography-high resolution mass-spectrometry (UHPLC-HRMS). Dyssynchrony induced low septal and high lateral asymmetry in workload and glucose-uptake. After 8 weeks, DHF animals exhibited LV dilation and LVEF decline (31.1 ± 5.1% vs. 59.4 ± 3.5% at baseline, $P < .05$). Septal thinning and lateral hypertrophy rebalanced workload and glucose-uptake. No fibrosis was seen on LGE or histology. DHF-animals showed enrichment of mitochondria at the intercalated discs (EMID-sign)—highest in the lateral wall (DHF septal 7.0 ± 4.8% vs. lateral 48.4 ± 12.3%, $P < .05$). Mitochondrial redox balance in DHF shifted towards a more oxidized state without evidence of oxidative stress. Metabolomics revealed no differences between septal and lateral walls but severe energy depletion of tricarboxylic acid cycle substrates and phosphocreatine in DHF (fold change DHF/CTRL 0.01, $P < .01$).

* Corresponding author. Tel: +49 941 944 0, Fax: +49 941 944 7213, Email: alexander.dietl@ukr.de
† Jens-Uwe Voigt and Jürgen Duchenne contributed equally to this work.

Conclusion Experimental DHF is characterized by non-fibrotic, dilated LV without signs of oxidative stress. Workload increase in the lateral wall leads to hypertrophy and EMID, homogenizing metabolic profiles between wall segments. However, the ventricle enters energy starvation and systolic dysfunction.

Graphical Abstract

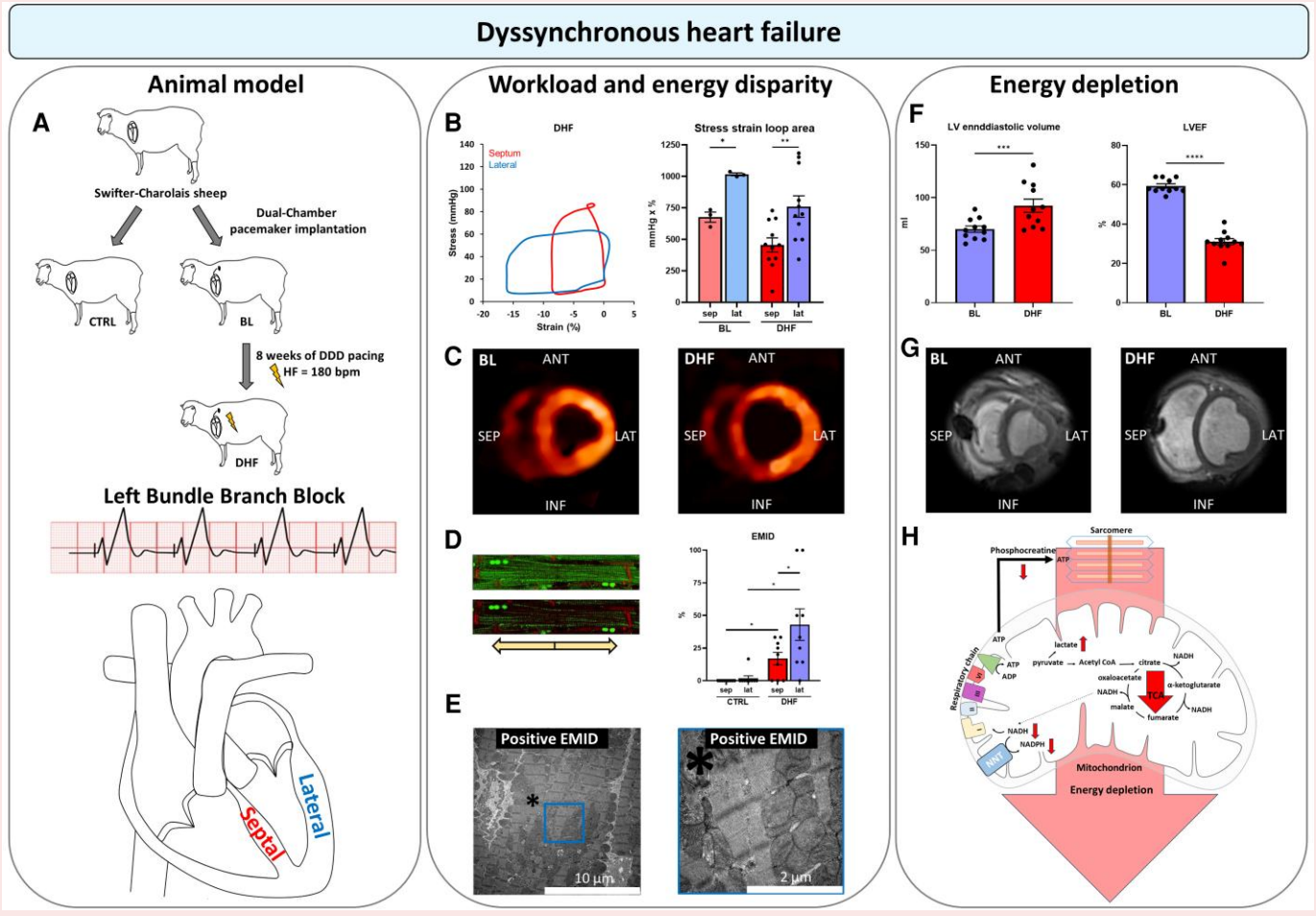

Cardiac dyssynchrony induces regional workload and energy disparities. These are mitigated by regional remodelling and mitochondrial adaptations, which ultimately fail to prevent heart failure and energy starvation. Fibrosis is absent, allowing for possible reversibility. In an ovine model of dyssynchronous heart failure (A), dyssynchronous left ventricular contraction immediately increased both the workload (B) and energy demand (C) of the more loaded lateral wall segments. Under increased workload, mitochondria shifted from the sarcomeres to the intercalated discs, a phenomenon referred to as the EMID-sign, predominantly found in lateral wall segments (D, E). Sustained dyssynchrony increased left-ventricular end-diastolic volume and reduced ejection fraction (F, G), associated with significant metabolic depletion (H). This was evidenced by substantial reductions in tricarboxylic acid cycle intermediates, NADH, and the phosphocreatine shuttle. Notably, cardiometabolic remodelling occurred in the absence of fibrosis, as confirmed by both MRI scans and histological analyses in dyssynchronous heart failure. BL: baseline. CTRL: control. DHF: dyssynchronous heart failure. HF: heart frequency. LV: left ventricular. LVEF: left ventricular ejection fraction. EMID: Enrichment of mitochondria at the intercalated discs. NADH: nicotinamide adenine dinucleotide. NADPH: nicotinamide adenine dinucleotide phosphate. TCA: tricarboxylic acid cycle. ANT: anterior. INF: inferior. LAT: lateral. SEP: septum.

Keywords Mitochondria • Heart failure • Dyssynchrony • Workload • Regional energy demand

Introduction

Left bundle branch block (LBBB)-induced dyssynchronous left ventricular (LV) contraction precipitates systolic dysfunction to dyssynchronous heart failure (DHF) or exacerbates pre-existing heart failure.[1] A critical consequence of LV dyssynchrony is the development of significant regional workload disparities. The early-activated interventricular septum becomes relatively underloaded, while the late-activated lateral LV wall is subjected to systolic pre-stretch and overloading.[1] Although these workload imbalances have been recognized for

decades, the associated energetic remodelling at the cellular and mitochondrial levels remains poorly understood. Mitochondria are critical for cardiac energy production and act as signalling hubs through emission of reactive oxygen species (ROS).[2,3] Distinct metabolic fingerprints have been identified in different heart failure aetiologies.[4] Yet, while global metabolic changes have been observed before, the precise regional metabolic alterations induced by dyssynchronous contraction have not been fully elucidated.

Based on the potential therapeutic impact of energetic remodelling in DHF, the present study employed an experimental ovine model to provide a comprehensive understanding of regional energetic remodelling. Mechanistic insights into mitochondrial dysfunctions may broaden the therapeutic armoury in DHF, as mitochondrial tasks are potentially targetable by different compounds.[2] Given the high burden of heart failure[5,6] and the role of dyssynchrony as a major driver of declining systolic function, enhanced insights into histological and ultrastructural remodelling may also improve prognostication and might guide the timing of interventions, such as cardiac resynchronization therapy.[1] Importantly, studying these mechanisms in a large-animal model offers high translational potential, providing a closer approximation to human physiology. Thus, further analyses of regional metabolism in the setting of DHF are urgently needed.

Our study aimed to evaluate mitochondrial distribution, energetics, redox-balance and reactive oxygen species (ROS)-signalling in experimental DHF. For this purpose, we used a sheep model with LBBB-like dyssynchrony caused by right ventricular pacing. We investigated LV morphology, function and metabolism by echocardiography, cardiac magnetic resonance imaging (MRI) and positron emission tomography, to quantify regional work and energy consumption. We analysed histology of mitochondrial remodelling in the identified wall segments with decreased and increased workload and energy demand. Further mitochondrial tasks were analysed by a systems medicine approach depicting the first integrative picture of mitochondrial remodelling in experimental DHF.

Methods

An expanded methods section can be found in the online supplementary material.

Animal model and experimental protocol

Eleven female Swifter-Charolais sheep (mean age of 12 months) underwent implantation of a DDD pacemaker with epicardial leads to induce an LBBB-like activation pattern. The implantation procedure has been described previously.[7,8] Following implantation, all animals were paced at 180 bpm for 8 weeks to induce DHF with LV remodelling. Baseline measurements were obtained in three animals, and in all animals after 8 weeks. All measurements were obtained at a fixed pacing rate of 110 bpm under apnoea with isoflurane anaesthesia. Six untreated sheep served as controls (CTRL). The Animal Ethics Committee of KU Leuven approved the study (project number P146/2012) and complies with the European Commission Directive 2010/63/EU for protection of animals used for scientific purposes. An overview of the experimental setup is provided in Online Supplementary Figure S1.

Echocardiographic and haemodynamic assessments

Short-axis echocardiography images at the mid-ventricular level enabled assessment of septal and lateral wall thickness and circumferential strain. LV haemodynamics were measured using a micromanometer-tipped pressure-volume catheter. Septal and lateral myocardial work, calculated from stress-strain loops, were derived via invasive pressure data combined with dynamic wall thickness, curvature and strain data obtained through echocardiography.

Magnetic resonance imaging and positron emission tomography

LV systolic function was evaluated by MRI on a 3T scanner using cine short-axis imaging. Late gadolinium enhancement (LGE) was determined to assess myocardial fibrosis. Additionally, septal and lateral myocardial glucose uptake was quantified with 18F-fluorodeoxyglucose (FDG) positron emission tomography and computed tomography (PET/CT). After an overnight fast and during a hyperinsulinaemic euglycaemic clamp, FDG was injected, which was followed by a CT scan for attenuation correction and a 30-minute PET emission scan. Electrocardiogram and respiratory data were recorded for subsequent motion correction.

Myocardial tissue collection and histology

At the study's conclusion, animals were sacrificed under isoflurane anaesthesia with intravenous pentobarbital. Myocardial tissue samples from mid-ventricular septal and lateral walls were collected and immediately either snap-frozen in liquid nitrogen for molecular analyses or fixed in formaldehyde and paraffin-embedded for histological and immunofluorescence analyses. Sections were stained with Sirius Red and TUNEL (terminal deoxynucleotidyl transferase dUTP nick end labelling) assays to assess collagen deposition and apoptosis, respectively. Fluorescence and confocal microscopy were performed using specific markers (e.g. heat shock protein 60 [HSP60] and N-Cadherin). The presence of the EMID-sign was quantified in a blinded manner by an investigator unaware of the treatment allocation. ImageJ (version 1.54g) was used for image visualization and signal assessment. For EMID-sign detection, a composite image of the red and green fluorescence channels was generated. The minimum threshold of the green channel was progressively increased using the Brightness/Contrast adjustment tool, until the green fluorescence either diminished uniformly, indicating absence of the EMID-sign, or persisted exclusively around the intercalated discs, indicating a positive EMID-sign (*Figure 4A and B*).

Biochemical, molecular, and metabolomic analyses

Mitochondrial redox state was evaluated by measuring nicotinamide adenine dinucleotide ratios ($NADH/NAD^+$) using a fluorometric assay, while tissue redox state was determined through glutathione (GSH/GSSG) assessments via colorimetric methods. For metabolomics, frozen tissue samples were homogenized and extracted in a 50:50 acetonitrile:water solution.[4] Extracts were analysed using ultra-high-performance liquid chromatography (UHPLC) coupled with a high-resolution mass spectrometer (HRMS) operating in both positive and negative ion modes.[4] Rigorous quality control procedures were applied, and metabolites were identified based on established databases.

Enzyme activities

Small frozen septal and lateral wall tissue samples were homogenized, and enzymatic activities of isocitrate dehydrogenase (IDH), aconitase, and citrate synthase (CS) were assessed spectrophotometrically at 340 nm or 412 nm using a Tecan Infinite plate reader. Proteins from whole tissue lysates were separated by SDS–PAGE, transferred to PVDF membranes, and detected using standard western blot procedures with HRP-conjugated antibodies and ECL-based chemiluminescence. Signal intensities were quantified using Image Lab 6.0.

Transmission electron microscopy

Eleven frozen cardiac muscle samples were fixed, resin-embedded, longitudinally sectioned, post-stained, and analysed by transmission electron microscopy in 30 areas around intercalated discs per sample.

Statistical analysis

Data are expressed as mean ± SEM. Differences between groups were assessed using paired or unpaired t-tests with $P < .05$ considered significant. Metabolomics data were median-normalized, log-transformed, and evaluated for normality and homoscedasticity. Multivariate analyses, including principal component analysis (PCA), analysis of variance (ANOVA), and

multivariate analysis of variance (MANOVA), were performed using R and GraphPad Prism 10.1.2 software.

Results

Dyssynchrony induces left ventricular eccentric, non-fibrotic remodelling, and systolic failure

First, we aimed to characterize cardiac remodelling in DHF. Right ventricular pacing induced dyssynchronous, LBBB-like LV contraction, visualized by echocardiography. After 8 weeks of dyssynchronous contraction, lateral wall thickness increased, whereas the thickness of the septal wall was decreased (*Figure 1A and B*). LV end-diastolic volume enlarged, whilst ejection fraction worsened (*Figure 1C and D*). Together, cardiac remodelling in DHF demonstrated eccentric hypertrophy, with septal thinning and lateral wall hypertrophy.

To assess cardiac fibrosis, cardiac MRI was performed in a total of 11 sheep after 8 weeks of RV-pacing. The imaging protocol included late acquisition of images following the injection of Gadolinium-based contrast media. Thus, a relevant late gadolinium enhancement in DHF was ruled out (*Figure 1E and F*), rendering myocardial fibrosis very unlikely. In line, the amount of collagen fibres visualized by Sirius Red staining was equal in CTRL and DHF (*Figure 1G–I*). The absence of fibrosis is paralleled by a modest or equal apoptotic rate in DHF (*Figure 1J*). Additionally, the ratio of the glutathione redox couples as surrogate of oxidative stress was fairly equal in control and DHF specimen (*Figure 1K*).

In summary, LBBB-like, right ventricular pacing-induced remodelling is characterized by LV dilatation, hypertrophy of the lateral wall segments concomitant with septal thinning and systolic dysfunction. Neither evidence of oxidative stress nor fibrosis is found in DHF.

Dyssynchrony-induced regional workload disparities drive specific, localized metabolic remodelling in dyssynchronous heart failure

Next, we investigated whether the observed regional remodelling in DHF is associated with regional ventricular workload and energy demand. Therefore, we performed echocardiography to derive stress-strain loops and FDG-PET to determine septal and lateral workload and glucose uptake at baseline and after 8 weeks. Following organ harvest, we analysed metabolite profiles from DHF hearts and compared them to CTRL hearts, by means of UHPLC-HRMS, separately examining septal and lateral wall segments.

Stress strain loop areas were calculated to derive septal and lateral myocardial work. Inducing dyssynchrony at baseline caused a workload asymmetry, with low septal and high lateral wall workload (*Figure 2A and C*) and glucose-uptake (*Figure 2D and F*). After DHF development, septal thinning and lateral hypertrophy caused a more homogenized distribution of septal and lateral wall workload (*Figure 2B and C*) and glucose uptake (*Figure 2E and F*), while the hypertrophied lateral wall retained higher workload and glucose uptake compared to the septal wall.

Principal component analysis of metabolite profiles further highlighted profound differences between CTRL and DHF hearts, while septal and lateral walls became more similar following remodelling (*Figure 2I*). Specifically, 276 metabolites were consistently identified with sufficient analytical quality by UHPLC-HRMS and subjected to further statistics, revealing considerable differences between DHF and CTRL tissue (*Figure 2G and H*), without overt discrepancies between septal and lateral wall. Intermediates of the tricarboxylic cycle (α-ketoglutarate, fumaric acid) and its link to oxidative phosphorylation and antioxidative capacity (reduced forms of nicotinamide adenine dinucleotide, NADH, and nicotinamide adenine dinucleotide phosphate, NADPH) were remarkably decreased in DHF compared with CTRL. ATP is transferred from mitochondria to the myofibrils by the creatine kinase system with phosphocreatine as shuttle, being a mainstay of cardiomyocyte energy transport and buffer systems.[9] The phosphocreatine pool of both, septal and lateral specimen, was emptied to one hundredth in DHF compared with control (*Figure 2J and K*). A shift of the mitochondrial redox balance ($NADH/NAD^+$) to a more oxidized state in DHF was an additional marker of mitochondrial energy depletion (*Figure 2L*). Unbiased, comprehensive pathway analyses of metabolomic profiles confirmed severe mitochondrial energy starvation in DHF compared with CTRL, as summarized in *Figure 3*. The complete set of significant metabolic alterations is provided in Online Supplementary Tables S1 and S2.

Our metabolomic analyses revealed that regional remodelling in the left ventricle led to a rather complete metabolic equalization between the lateral wall and the septum, consistent with the homogenization of glucose uptake observed in PET imaging. However, a striking difference was observed in the depletion of high-energy substrates in the DHF group compared to CTRL. To explore potential enzymatic correlates underlying the reduction in TCA intermediates and the marked decrease in phosphocreatine levels, we performed targeted exploratory analyses of selected mitochondrial enzymes and respiratory chain components. Measurements of citrate synthase, aconitase, and isocitrate dehydrogenase activities revealed no detectable differences between wall segments or experimental groups (Online Supplementary Figure S2A–C). Likewise, protein abundance of respiratory chain complexes remained comparable across ventricular regions and conditions (Online Supplementary Figure S2D–J). Together, these analyses were consistent with preserved enzyme activities and respiratory chain protein abundance despite profound alterations in the cardiac metabolome.

In summary, dyssynchrony immediately increased workload and glucose uptake in the lateral wall compared to the septum. Over eight weeks of remodelling, workload and glucose uptake distribution became more even. Metabolomic analyses revealed that DHF hearts suffer from a global severe mitochondrial energy depletion, as evidenced by decreased TCA cycle intermediates, a dramatically reduced phosphocreatine pool, and a shift toward an oxidized mitochondrial redox state—without overt differences between the septal and lateral wall.

Chronic dyssynchrony is associated with a shift of mitochondria away from the sarcomeres towards the intercalated discs (EMID-sign)

Based on the echocardiographic and PET findings, we sought to explore how mitochondria reorganize in order to meet the challenges of dyssynchronous workload conditions and energy demand. For further analyses, we focused on the septal and lateral wall segments, as these showed the most pronounced differences in hypertrophy, workload and energy demand. We examined mitochondrial distribution in DHF using confocal microscopy. Deparaffinized LV slices were incubated with antibodies against HSP60 (green fluorescence) to identify mitochondria and against N-Cadherin (red fluorescence) to visualize the intercalated discs (*Figure 4A and B*).

Confocal laser scanning images were analysed for enrichment of mitochondria at the intercalated discs (EMID-sign), which was assessed by a researcher unaware of the treatment groups. Dyssynchrony-induced workload increase led to a higher occurrence of EMID in DHF, with a more pronounced effect observed in the lateral wall segments compared to the septum (DHF septal mean $17.0 \pm 4.8\%$ vs. lateral $48.4 \pm 12.3\%$, $P < .05$, *Figure 4C and D*). Transmission electron microscopy indicated that this redistribution corresponded ultrastructurally to a numerical

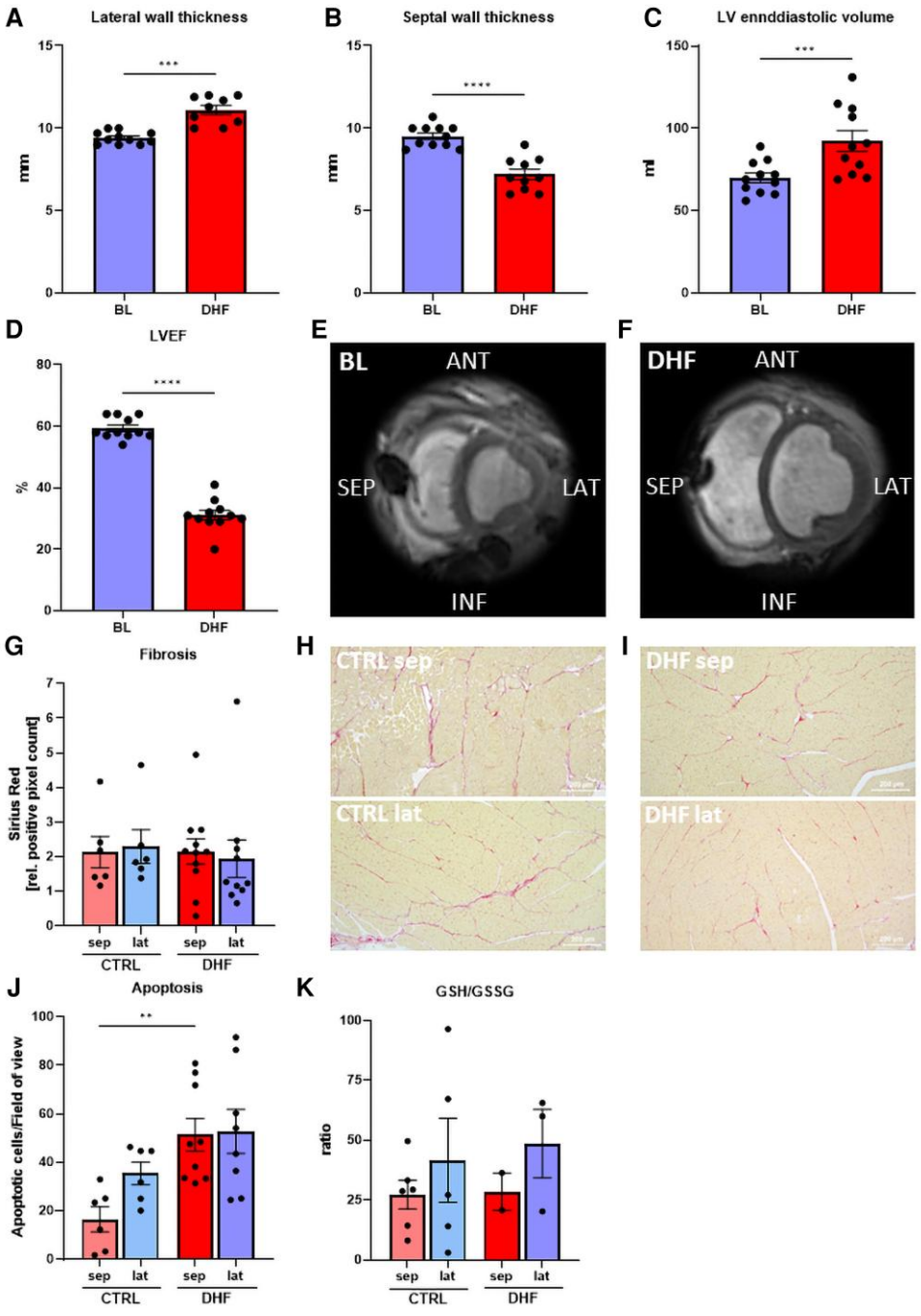

Figure 1 Dyssynchrony leads to left ventricular dilatation, regional hypertrophy and reduced systolic function in the absence of oxidative stress and fibrosis

LBBB-like left ventricular contraction led to systolic dysfunction, septal thinning, lateral hypertrophy and LV-dilatation (A–D; $n = 10$–11) displayed by echocardiography. After remodelling the dilated left ventricle showed a thinned septum and thickened lateral wall. Gadolinium enhancement (LGE) was absent before and after remodelling (E, F). In line, ultrastructural analyses showed similar amounts of fibrosis mirrored by Sirius Red staining in control (CTRL; $n = 6$) and DHF animals (G–I; $n = 11$–12). In septal wall tissue, apoptosis was slightly increased (J; CTRL $n = 6$, DHF $n = 8$–9). DHF does not imply oxidative stress (by terms of glutathione-oxidation; K; CTRL $n = 5$–6, DHF $n = 2$–3). Data are shown as mean ± SEM, $^{*}P < .05$, $^{**}P < .01$, $^{***}P < .001$, $^{****}P < .0001$. BL: baseline. CTRL: control. DHF: dyssynchronous heart failure. LV: left ventricular. LVEF: left ventricular ejection fraction. ANT: anterior. INF: inferior. LAT: lateral. SEP: septum. GSH: glutathione. GSSG: glutathione disulphide.

accumulation of mitochondria, without megamitochondria or cristae malformations (*Figure 4E–H*).

Overall, chronic ventricular dyssynchrony disrupts the mitochondrial-sarcomeric cluster in DHF, particularly in the relatively overloaded and hypertrophied lateral wall. The pre-stretch-induced increase in lateral workload is associated with the EMID-sign, suggesting a longer distance between mitochondrial energy supply and sarcomeric breakdown.

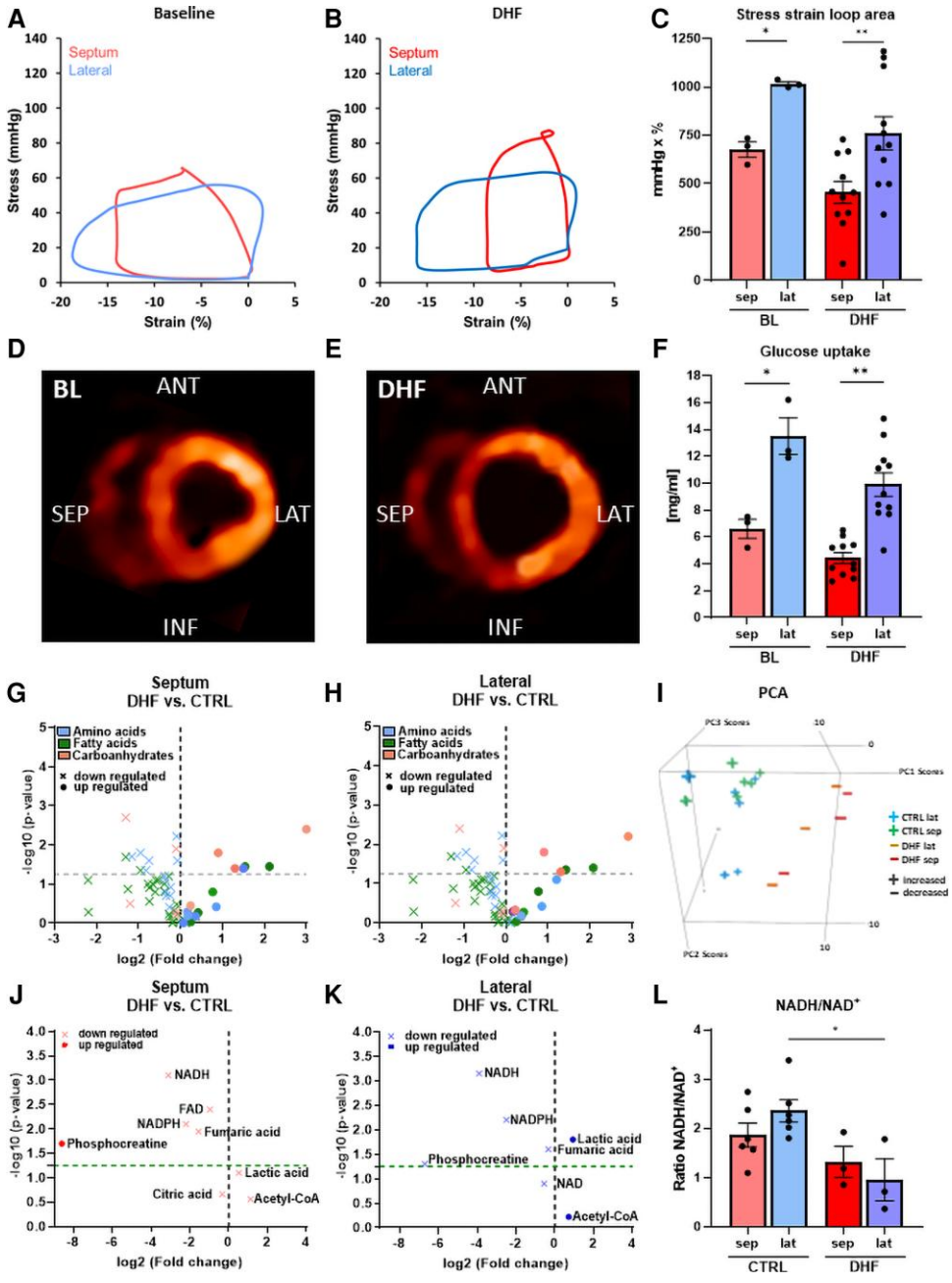

Figure 2 Regional workload imbalance and metabolic remodelling in DHF

In DHF, lateral wall segments exhibited an immediate increase in mechanical workload and glucose uptake compared to septal segments, as reflected in stress strain loops (A–C; BL $n = 3$, DHF $n = 11$) and FDG-PET imaging (D–F; BL $n = 3$, DHF $n = 11$). During the eight weeks of remodelling, lateral hypertrophy partially reduced regional disparities in workload and glucose uptake but did not fully equalize them (A–F). Principal component analysis (PCA) revealed that the primary metabolic distinction was between DHF and control tissues (I), while the profiles of septal and lateral wall segments were largely equivalent (G, H). The entire left ventricle ultimately succumbed to energy depletion, evidenced by severe phosphocreatine loss in septal and lateral wall segments (J, K) and a shift in mitochondrial redox balance toward a more oxidized state (L; CTRL $n = 6$, DHF $n = 3$). (C, F, L) Data are shown as mean ± SEM, $^{*}P < .05$, $^{**}P < .01$. BL: baseline; CTRL: control; DHF: dyssynchronous heart failure (after 8 weeks); LV: left ventricular; LVEF: left ventricular ejection fraction; ANT: anterior; INF: inferior; LAT: lateral; SEP: septum; NADH: nicotinamide adenine dinucleotide.

Discussion

Our study examined the interplay of LV myocardial, energetic, and mitochondrial remodelling in an animal model of chronic ventricular dyssynchrony. Dyssynchrony immediately induced a septal-to-lateral wall asymmetry in stress-strain loop area, with decreased septal loading and increased lateral loading—the latter due to early-systolic pre-stretch and subsequent amplified systolic shortening. This mechanistic pattern is well in line with the pathophysiology observed in patients with LBBB.[10] In parallel, a septal-to-lateral wall asymmetry in glucose energy consumption was confirmed by PET scans, with highest metabolism in the lateral wall. This adverse asymmetry in loading and energy demand precipitated a distinct eccentric, dilated, and non-fibrotic LV remodelling over eight weeks of dyssynchronous pacing. Notably, neither oxidative stress nor fibrosis was detected by MRI or histological analysis, a finding that may underlie the reversibility of dyssynchronous

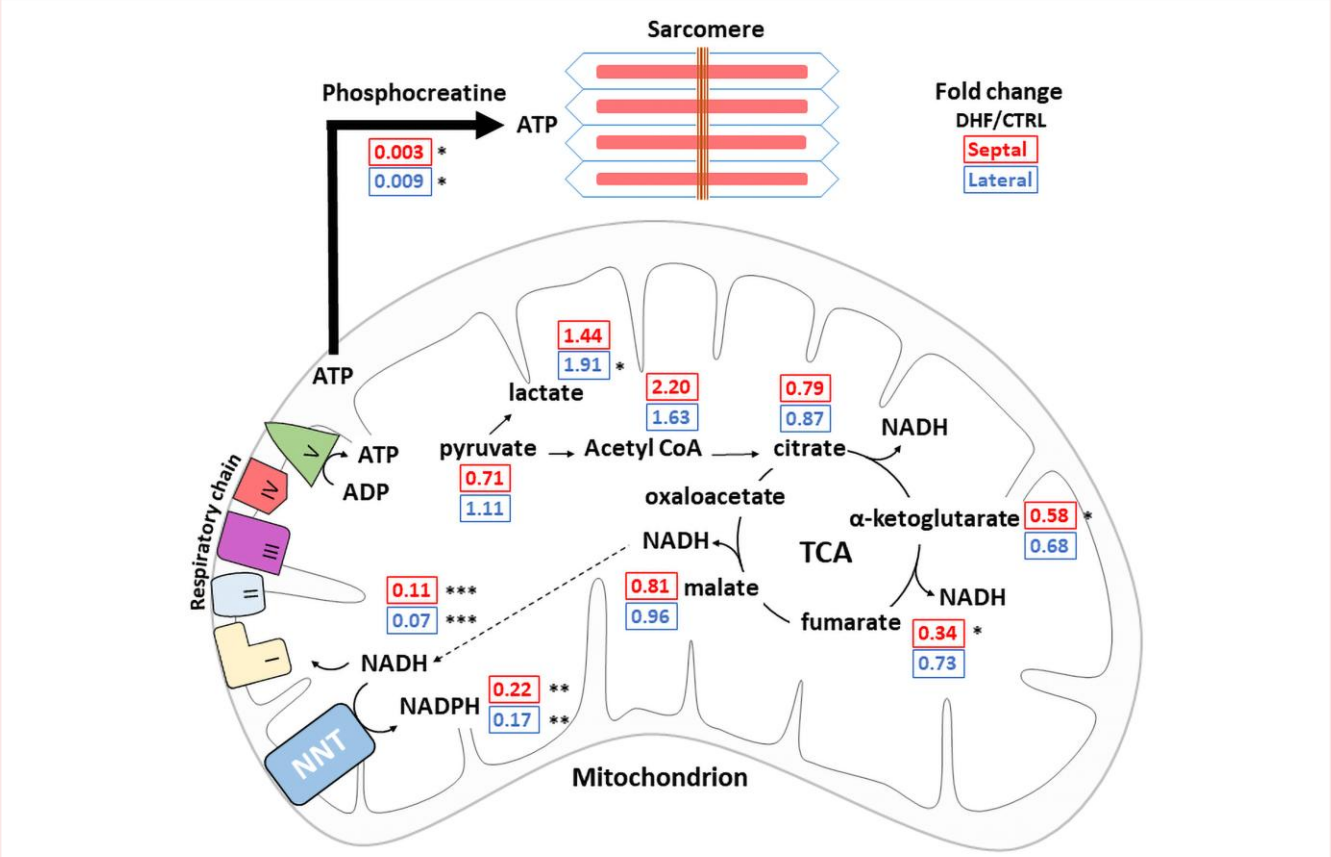

Figure 3 Metabolic pathway analysis reveals severe mitochondrial energy depletion in DHF

Illustration of metabolite profiles with fold change lateral and septal CTRL vs. DHF showing a reduction of TCA substrates, NADH/NADPH pools and phosphocreatine decrease in septal and lateral wall segments in DHF. Data are shown with *$P < .05$, **$P < .01$, ***$P < .001$ for *t*-test. CTRL: control; DHF: dyssynchronous heart failure; NADH: nicotinamide adenine dinucleotide; NADPH: nicotinamide adenine dinucleotide phosphate; ATP: adenosine triphosphate; ADP: adenosine diphosphate; TCA: tricarboxylic acid cycle.

remodelling under resynchronization therapy.[7,11,12] In response to the increased energetic demand, mitochondria reoriented their network away from the sarcomeres toward the intercalated discs. This EMID-sign, previously reported exclusively in tachycardiomyopathy,[4,13] was also observed in our experimental DHF model, but now with a distinct septal-to-lateral asymmetry, clearly reflecting the regional workload and metabolic asymmetry induced by dyssynchrony. Our findings suggest that EMID appears to be part of a stretch-induced remodelling process, which appear 'globally' across the LV of the DHF heart—due to LV dilatation (and thus stretch) and systolic dysfunction—as well as show marked regional differences in experimental DHF—due to lateral wall pre-stretch, overloading and hypertrophy.

Dyssynchrony-induced remodelling

In a healthy heart, electrical impulses propagate through the bundle branches and Purkinje fibres to ensure synchronous ventricular contraction. LBBB disrupts this conduction, leading to dyssynchronous contraction, where the right ventricle and septum activate first, followed by the LV lateral wall. Thus, the ventricular septum is activated during isovolumetric contraction, before the aortic valve opens, decreasing septal and increasing lateral wall workload.[1]

Our findings indicate that dyssynchronous remodelling follows regional workload distribution and energy demand at macroscopic and cellular levels. The process of septal wall thinning and lateral wall hypertrophy caused by LBBB eventually leads to a more homogeneous distribution of work per myocardial volume unit. Metabolomic analyses confirmed hypertrophy as a sufficient compensatory mechanism, as metabolite profiles between lateral and septal walls converged after eight weeks. However, despite these adaptations, energy depletion progressed throughout the entire LV, ultimately associated with systolic heart failure. Mitochondrial energy depletion is associated with starved cardiomyocytes, with phosphocreatine levels diminished to nearly one hundredth of control values.[9] ATP is not directly transported from mitochondria to the sarcomeres, but mitochondrial ATP converts creatine to phosphocreatine, which is a very high-energy compound and diffuses from mitochondria to the sarcomeres.[9] Reductions in phosphocreatine were reported in dyssynchronous, but not synchronous, pacing-induced heart failure in a canine model.[14] Consistent with this energetic susceptibility, right-ventricular pacing-induced dyssynchrony alters metabolic signalling and increases cellular stress responses.[15] Taken together with these data, our results reinforce the view that dyssynchronous activation inherently predisposes the myocardium to energetic starvation.

Against expectations, oxidative stress did not increase in experimental DHF, despite high workload and fast running glucose-catabolism in lateral wall segments. When ROS production overwhelms the antioxidative system in canonical heart failure pathophysiology, oxidative stress evolves and ROS damage the cells, increase apoptosis and induce fibrosis.[2] As no evidence of oxidative stress was detected, neither MRI nor histology found fibrosis in experimental DHF. The distinct

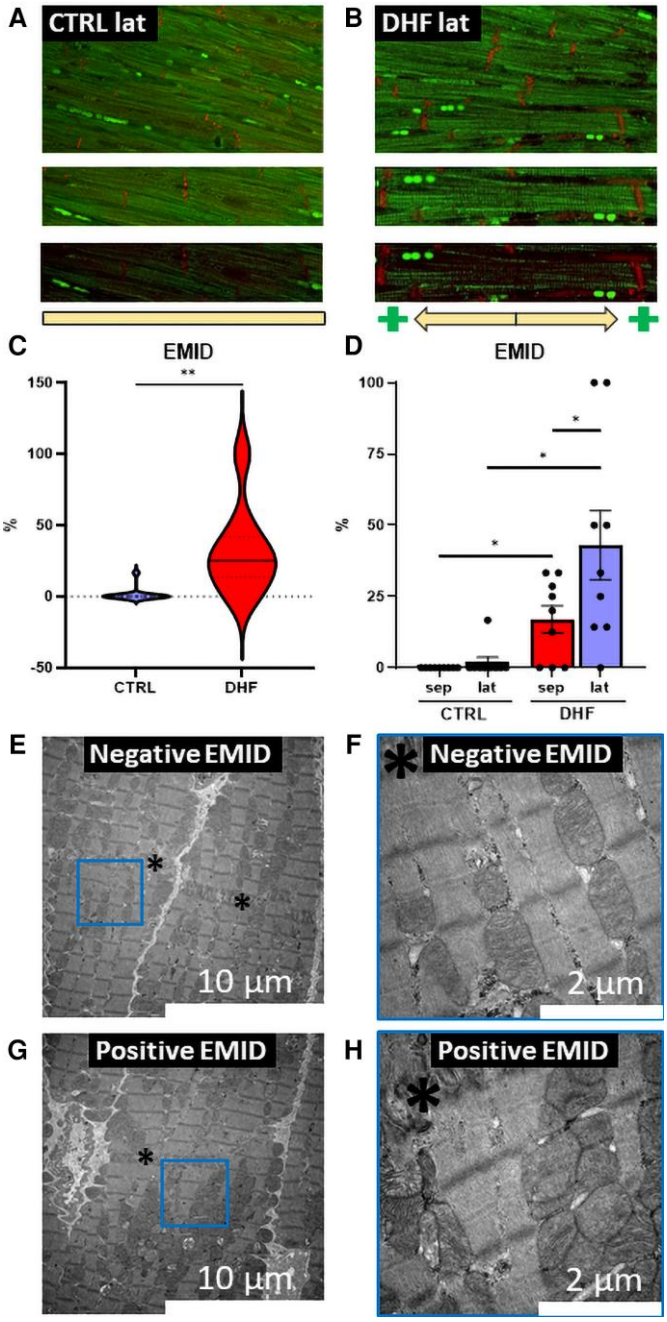

Figure 4 Regional mitochondrial remodelling in DHF

Confocal microscopy revealed a redistribution of mitochondria (green, HSP60) towards the Z-lines (red, N-cadherin) in DHF, whereas in control animals mitochondria were homogeneously distributed along the sarcomeres. (A, B) Top: composite image of red and green fluorescence channel. Middle: zoom on a single cardiomyocyte. Bottom: progressive increase of the green channel threshold to reveal absence (uniform loss, A) or presence (localization at intercalated discs, B) of the EMID-sign. The mitochondrial shift to the intercalated discs (Enrichment of mitochondria at the intercalated discs, EMID-sign) was more pronounced in mitochondria derived from DHF animals` lateral wall segments than in septal segments (C, D; CTRL $n = 6$, DHF $n = 8$–9). Transmission electron microscopy revealed that this redistribution corresponded to numerical accumulation of mitochondria, without formation of megamitochondria or cristae abnormalities (E–H). Data shown as mean ± SEM, *$P < .05$ for *t*-test. Panel F and H: higher magnification views of the blue-boxed regions in panels E and G. * intercalated discs; CTRL: control; DHF: dyssynchronous heart failure; LAT: lateral. SEP: septum.

metabolic and structural characteristics of DHF underscore the need to rethink the pathophysiological mechanisms driving this condition. The emphasis on oxidative stress in conventional models of heart failure does not adequately explain the features of DHF. The lack of irreversible ROS-damage may contribute to the reversibility of DHF. However, this reversibility might possibly be limited to a certain time interval. While our study conducted dyssynchronous pacing for eight weeks, longer duration of dyssynchrony have been reported to eventually cause the appearance of myocardial fibrosis.[15]

EMID-sign

Further examination of the mitochondrial network revealed a striking shift towards the intercalated discs in the more loaded lateral wall

segments of the DHF hearts, resulting in a longer physical distance between mitochondrial energy supply and sarcomeric breakdown in the lateral wall.

This EMID-sign, initially identified in tachycardiomyopathy biopsies,[13] was later validated in a rapid-pacing animal model.[4] In our study, EMID emerged independently of oxidative stress, suggesting that energy depletion, rather than oxidative damage, underlies this phenomenon. Previous research in tachycardiomyopathy supports this notion.[4] Thus, EMID appears to reflect a LV-wide energy depletion in DHF, with highest values in the lateral wall, paralleled by workload-induced hypertrophy rather than oxidative injury.

Dyssynchrony and tachycardiomyopathy

In tachycardiomyopathy, sustained high ventricular heart rates induce uniform LV dilation, decline of systolic function, neurohormonal activation, cachexia and mitochondrial exhaustion.[15–19] These changes remain largely reversible upon cessation of tachycardia.[20] In our ovine model, pacing-induced tachycardia was necessary to consistently override the intrinsic heart rhythm and establish permanent dyssynchronous contraction. Tachycardia must therefore be acknowledged as a potential contributing factor when considering our results. However, dyssynchrony led to a distinctly regional remodelling, where increased workload in the late-activated lateral wall triggered structural remodelling in the form of hypertrophy, accompanied by a markedly greater abundance of EMID in the lateral segments, which has not been previously described.

While DHF and tachycardiomyopathy culminate in global energy depletion, only DHF exhibits the pronounced septal-lateral heterogeneity in workload, substrate utilization and mitochondrial distribution that we report. This region-specific metabolic remodelling further sets DHF apart from other heart-failure aetiologies as ischaemic, pressure-overload, hypertrophic and dilated cardiomyopathy, which typically manifest diffuse oxidative stress, apoptosis and fibrosis.[4,21–24]

Overlapping pathophysiological mechanisms in DHF and tachycardiomyopathy are of considerable clinical significance in the commonly encountered context of concomitant tachycardia and LBBB. In tachycardiomyopathy, tissue hypoxia has increasingly been implicated as a key driver of specific metabolic remodelling, particularly myocardial energy depletion.[25] In experimental DHF, our findings provide evidence that the late-activated segments of the lateral ventricular wall are characterized by a significantly increased energy demand. To compensate, myocardial blood flow has been shown to be highest in the lateral walls of patients with LBBB and non-ischaemic cardiomyopathies[26]; however, this compensatory mechanism ultimately fails to satisfy the oxygen and metabolic substrate requirements. At elevated heart rates, coronary perfusion and oxygen supply become increasingly insufficient, further compromising the delivery of oxygen and energy-supplying substrates to the lateral wall in the presence of LBBB.

Together, there are noteworthy parallels between DHF and tachycardiomyopathy in our model and in general. Yet, our findings revealed a uniquely regional signature of metabolic remodelling in DHF following regional workload disparities.

Translational outlook

In view of the substantial burden of heart failure and the contribution of dyssynchrony to progressive systolic dysfunction, our findings point towards translational opportunities in patients with DHF. Our results on EMID-sign are a relevant step in translational medicine. Previously described solely in tachycardiomyopathy,[4,13] our study demonstrates that EMID follows stretch-induced workload increases in dyssynchronous hearts. Though the presence of EMID in human biopsies was considered to confirm tachycardiomyopathy diagnosis,[13] our results challenge the notion of EMID as a definitive marker for tachycardiomyopathy. EMID may also arise in lateral wall biopsies from other heart failure entities with conduction delays. Notably, the EMID-sign has to date been observed exclusively in non-fibrotic cardiomyopathies,[4,13] suggesting that they could serve as markers of reversibility. Thus, EMID and regional energetic patterns might provide measurable markers that indicate the potential for functional recovery, for example by helping to distinguish likely responders from non-responders to cardiac resynchronization therapy. Another example could be cardiogenic shock, where these markers might support early assessment of reversibility, which is a key prerequisite for bridging to recovery and for guiding the use of mechanical circulatory support,[27] particularly given the limited evidence for such support in end-stage heart failure.[28]

Together, our data provide a basis for future clinical research, pinpointing EMID-sign as a marker or even prognostic tool in DHF and increasing the knowledge on histologic diagnosis of tachycardiomyopathy.

Limitations of the study

Right ventricular pacing may slightly differ from the conduction pattern in left bundle branch block.[29] Despite subtle differences in conduction, right ventricular pacing is still commonly believed to provoke comparable hemodynamic and ultrastructural effects as seen in DHF.[1]

The imaging part of this study was originally designed to compare baseline status and remodelled hearts after eight weeks of dyssynchronous pacing, without the need for control animals. As a result, no imaging or hemodynamic data were collected in the control animals. Nevertheless, notable cardiac pathology was considered to be unlikely in healthy, untreated sheep, thus allowing the comparison with tissue of DHF animals.

We did not directly measure ROS levels (e.g. superoxide amount) but assessed indirect surrogate markers, such as glutathione oxidation and aconitase activity. However, a downstream effect of oxidative injury was rigorously evaluated via comprehensive fibrosis assessment. The absence of fibrosis in cardiac MRI and histology argues against relevant oxidative damage

Targeted mitochondrial functional follow-up analyses presented in the Online Supplementary Information were performed with a limited sample size and therefore warrant cautious interpretation. These experiments should be viewed as exploratory observations that complement the primary metabolomic findings.

Conclusions

Dyssynchrony induces left ventricular dilation without evidence of oxidative stress or fibrosis. Early septal contraction increases stretch-induced workload and energy demand in the late-activated lateral wall segments. The resulting morphological and metabolic remodelling aligns with these regional workload and energy demands, with lateral wall segments exhibiting hypertrophy and mitochondrial redistribution to intercalated discs. In the remodelled hearts, metabolite profiles level up between septal and lateral walls. However, the entire ventricle goes finally into energy starvation and systolic dysfunction.

Dyssynchrony induces left ventricular dilation without oxidative stress or fibrosis. Early septal contraction raises workload and energy demand in the late-activated lateral wall segments. The ensuing morphological and metabolic changes mirror these regional demands: lateral segments develop hypertrophy and redistribute mitochondria toward the intercalated discs. Metabolite profiles become uniform between septal and lateral walls. Ultimately, the entire ventricle yields to energy starvation and systolic dysfunction.

Supplementary data

Supplementary data are available at *European Journal of Heart Failure* online.

Acknowledgements

The authors greatly appreciate the outstanding technical assistance of Gabriela Pietrzyk, Cristina Bravo-de-Laguna-Faber, Anja Sauer, Eva-Maria Prugger, and David Célis. The authors thank Mr. Heiko Siegmund for his support with the electron microscopy analyses and for his insightful and constructive discussion of the results.

Declarations

Disclosure of interest

A.D. received speaker honoraria from Johnson & Johnson. C.M. received honoraria for advisory boards and talks from AstraZeneca, Boehringer Ingelheim, Bristol Myers Squibb, Cytokinetics, Lilly, and Novo Nordisk.

Data availability

All data are incorporated into the article and its online supplementary material.

Funding

Parts of this work were supported by the Deutsche Forschungsgemeinschaft [DFG, German Research Foundation – DI 2876/2-1; 519332007 to A.D.] and a project grant of the KU Leuven [OT/12/084]. L.S.M. is supported by the Horizon Europe grant STRATIFY HF (project number 101080905) and the Deutsche Forschungsgemeinschaft [DFG, German Research Foundation MA 1982/11-1; and TRR 374 grant, project number: 509149993, TPA6]. C.M. received support by the Deutsche Forschungsgemeinschaft [DFG, German Research Foundation, SFB 1525 -project ID 453989101, MA 2528/8-1 project ID 505805397, and 9-2 project ID 315254108]. The Research Foundation Flanders (FWO) provided individual research support to J.D. [12ZZN22N] and J.U.V. [1832917N].

Ethical approval

Ethical approval was not required.

Pre-registered clinical trial number

None supplied.

References

1. Tan NY, Witt CM, Oh JK, Cha Y-M. Left bundle branch block: current and future perspectives. *Circ Arrhythm Electrophysiol* 2020;**13**:e008239. https://doi.org/10.1161/CIRCEP.119.008239
2. Dietl A, Maack C. Targeting mitochondrial calcium handling and reactive oxygen species in heart failure. *Curr Heart Fail Rep* 2017;**14**:338–49. https://doi.org/10.1007/s11897-017-0347-7
3. Birner C, Dietl A, Deutzmann R, Schröder J, Schmid P, Jungbauer C, *et al.* Proteomic profiling implies mitochondrial dysfunction in tachycardia-induced heart failure. *J Card Fail* 2012;**18**:660–73. https://doi.org/10.1016/j.cardfail.2012.06.418
4. Paulus MG, Renner K, Nickel AG, Brochhausen C, Limm K, Zügner E, *et al.* Tachycardiomyopathy entails a dysfunctional pattern of interrelated mitochondrial functions. *Basic Res Cardiol* 2022;**117**:45. https://doi.org/10.1007/s00395-022-00949-0
5. Savarese G, Becher PM, Lund LH, Seferovic P, Rosano GMC, Coats AJS. Global burden of heart failure: a comprehensive and updated review of epidemiology. *Cardiovasc Res* 2023;**118**:3272–87. https://doi.org/10.1093/cvr/cvac013
6. Heinrich MA, Stark KJ, Zimmermann ME, Herold JM, Brandl C, Schober AD, *et al.* NT-proBNP in the very old population: reference values and heart failure specificity from the AugUR-study. *Clin Res Cardiol* 2025. https://doi.org/10.1007/s00392-025-02785-3. Epub ahead of print.
7. Duchenne J, Turco A, Ünlü S, Pagourelias ED, Vunckx K, Degtiarova G, *et al.* Left ventricular remodeling results in homogenization of myocardial work distribution. *Circ Arrhythm Electrophysiol* 2019;**12**:e007224. https://doi.org/10.1161/CIRCEP.118.007224
8. Duchenne J, Claus P, Pagourelias ED, Mada RO, van Puyvelde J, Vunckx K, *et al.* Sheep can be used as animal model of regional myocardial remodeling and controllable work. *Cardiol J* 2019;**26**:375–84. https://doi.org/10.5603/CJ.a2018.0007
9. Neubauer S. The failing heart–an engine out of fuel. *N Engl J Med* 2007;**356**:1140–51. https://doi.org/10.1056/NEJMra063052
10. Craine A, Krishnamurthy A, Villongco CT, Vincent K, Krummen DE, Narayan SM, *et al.* Successful cardiac resynchronization therapy reduces negative septal work in patient-specific models of dyssynchronous heart failure. *PLoS Comput Biol* 2024;**20**:e1012150. https://doi.org/10.1371/journal.pcbi.1012150
11. Moss AJ, Hall WJ, Cannom DS, Klein H, Brown MW, Daubert JP, *et al.* Cardiac-resynchronization therapy for the prevention of heart-failure events. *N Engl J Med* 2009;**361**:1329–38. https://doi.org/10.1056/NEJMoa0906431
12. Calle S, Duchenne J, Beela AS, Stankovic I, Puvrez A, Winter S, *et al.* Clinical and experimental evidence for a strain-based classification of left bundle branch block-induced cardiac remodeling. *Circ Cardiovasc Imaging* 2022;**15**:e014296. https://doi.org/10.1161/CIRCIMAGING.122.014296
13. Mueller KAL, Heinzmann D, Klingel K, Fallier-Becker P, Kandolf R, Kilias A, *et al.* Histopathological and immunological characteristics of tachycardia-induced cardiomyopathy. *J Am Coll Cardiol* 2017;**69**:2160–72. https://doi.org/10.1016/j.jacc.2017.02.049
14. Shibayama J, Yuzyuk TN, Cox J, Makaju A, Miller M, Lichter J, *et al.* Metabolic remodeling in moderate synchronous versus dyssynchronous pacing-induced heart failure: integrated metabolomics and proteomics study. *PLoS One* 2015;**10**:e0118974. https://doi.org/10.1371/journal.pone.0118974
15. Lin Y-S, Chen H-C, Lee W-C, Ho W-C, Chang S-F, Chen Y-L, *et al.* Effect of his bundle pacing on abnormal myocardial fatty acid and glucose metabolism induced by right ventricular pacing. *J Am Heart Assoc* 2024;**13**:e032386. https://doi.org/10.1161/JAHA.123.032386
16. Birner C, Ulucan C, Bratfisch M, Götz T, Dietl A, Schweda F, *et al.* Antihypertrophic effects of combined inhibition of the renin-angiotensin system (RAS) and neutral endopeptidase (NEP) in progressive, tachycardia-induced experimental heart failure. *Naunyn Schmiedebergs Arch Pharmacol* 2012;**385**:1117–25. https://doi.org/10.1007/s00210-012-0791-6
17. Dietl A, Winkel I, Deutzmann R, Schröder J, Hupf J, Riegger G, *et al.* Interatrial differences of basal molecular set-up and changes in tachycardia-induced heart failure-a proteomic profiling study. *Eur J Heart Fail* 2014;**16**:835–45. https://doi.org/10.1002/ejhf.122
18. Dietl A, Winkel I, Pietrzyk G, Paulus M, Bruckmann A, Schröder JA, *et al.* Skeletal muscle alterations in tachycardia-induced heart failure are linked to deficient natriuretic peptide signalling and are attenuated by RAS-/NEP-inhibition. *PLoS One* 2019;**14**:e0225937. https://doi.org/10.1371/journal.pone.0225937
19. Mayer MNS, Köhler LM, Paulus M, Iberl S, Heinrich M, Wagner S, *et al.* MATLAB-based methods allow precise, high-throughput quantification of nuclear morphology and texture in tachycardiomyopathy. *J Histochem Cytochem* 2025;**73**:115–28. https://doi.org/10.1369/00221554251332331
20. Martin CA, Lambiase PD. Pathophysiology, diagnosis and treatment of tachycardiomyopathy. *Heart* 2017;**103**:1543–52. https://doi.org/10.1136/heartjnl-2016-310391
21. Bertero E, Popoiu T-A, Maack C. Mitochondrial calcium in cardiac ischemia/reperfusion injury and cardioprotection. *Basic Res Cardiol* 2024;**119**:569–85. https://doi.org/10.1007/s00395-024-01060-2
22. Loescher CM, Breitkreuz M, Li Y, Nickel A, Unger A, Dietl A, *et al.* Regulation of titin-based cardiac stiffness by unfolded domain oxidation (UnDOx). *Proc Natl Acad Sci U S A* 2020;**117**:24545–56. https://doi.org/10.1073/pnas.2004900117
23. Schönmehl R, Mendelsohn DH, Winter L, Pabel S, Niedermair T, Evert K, *et al.* Comparative analysis of mitochondria surrounding the intercalated discs in heart diseases-an ultrastructural pilot study. *Int J Mol Sci* 2024;**25**:7644. https://doi.org/10.3390/ijms25147644
24. Kohlhaas M, Sequeira V, Parikh S, Dietl A, Richter O, Bay J, *et al.* Mitochondrial reactive oxygen species cause arrhythmias in hypertrophic cardiomyopathy. bioRxiv, https://doi.org/10.1101/2024.10.02.616214, 03 October 2024, preprint: not peer reviewed.
25. Tu C, Caudal A, Liu Y, Gorgodze N, Zhang H, Lam CK, *et al.* Tachycardia-induced metabolic rewiring as a driver of contractile dysfunction. *Nat Biomed Eng* 2024;**8**:479–94. https://doi.org/10.1038/s41551-023-01134-x
26. Prinzen FW, Auricchio A. The "missing" link between acute hemodynamic effect and clinical response. *J Cardiovasc Transl Res* 2012;**5**:188–95. https://doi.org/10.1007/s12265-011-9331-x
27. Lorusso R, Shekar K, MacLaren G, Schmidt M, Pellegrino V, Meyns B, *et al.* ELSO interim guidelines for venoarterial extracorporeal membrane oxygenation in adult cardiac patients. *ASAIO J* 2021;**67**:827–44. https://doi.org/10.1097/MAT.0000000000001510
28. Morici N, Sacco A, Frea S, Rota M, Villanova L, Gravinese C, *et al.* Early intra-aortic balloon support for heart failure-related cardiogenic shock: a randomized clinical trial. *J Am Coll Cardiol* 2025;**85**:1587–97. https://doi.org/10.1016/j.jacc.2025.03.003
29. Varma N. Left ventricular electrical activation during right ventricular pacing in heart failure patients with LBBB: visualization by electrocardiographic imaging and implications for cardiac resynchronization therapy. *J Electrocardiol* 2015;**48**:53–61. https://doi.org/10.1016/j.jelectrocard.2014.09.002